

Pyrrolyl-, 2-(2-thienyl)pyrrolyl- and 2,5-bis(2-thienyl)pyrrolyl-nucleosides: synthesis, molecular and electronic structure, and redox behaviour of C5-thymidine derivatives†

Miguel A. Galindo,^a Jennifer Hannant,^a Ross W. Harrington,^b William Clegg,^b Benjamin R. Horrocks,^a Andrew R. Pike^a and Andrew Houlton^{*a}

Received 21st July 2010, Accepted 11th November 2010

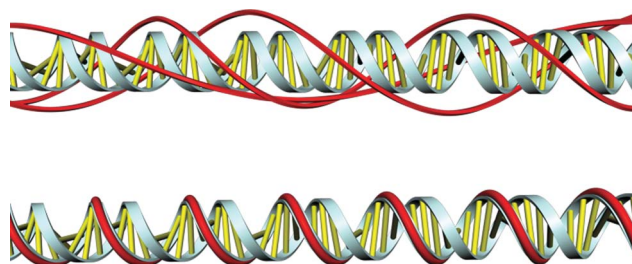
DOI: 10.1039/c0ob00466a

A series of modified nucleosides based on thymidine have been prepared by Pd-catalysed cross-coupling between *N*-alkyl-alkynyl functionalised pyrrolyl- (**py**), 2-(2-thienyl)pyrrolyl- (**tp**) or 2,5-bis(2-thienyl)pyrrolyl (**tpt**) groups with 5-iodo-2'-deoxyuridine. The length of the alkyl chain linking the nucleoside and pyrrolyl-containing unit, N(CH₂)_{*n*}C≡C-nucleoside (where *n* = 1–3) was also varied. The compounds have been characterised by ¹H NMR, ES-MS, UV-vis, cyclic voltammetry (CV) and, in some cases, single-crystal X-ray diffraction. Cyclic voltammetry studies demonstrated that all the **py**-, **tp**- and **tpt**-alkynyl derivatives **1–7** can be electrochemically polymerised to form conductive materials. It was found that increasing the *N*-alkyl chain length in these cases resulted in only minor changes in the oxidation potential. The same behaviour was observed for the **tp**- and **tpt**-modified nucleosides **9–12**; however, the **py**-derivative, **8**, produced a poorly conducting material. DFT calculations on the one-electron oxidised cation of the modified nucleosides bearing **tp** or **tpt** showed that spin density is located on the pyrrolyl and thienyl units in all cases and that the coplanarity of adjacent rings increases upon oxidation. In contrast, in the corresponding pyrrolyl cases the spin density is distributed over the whole molecule, suggesting that polymerisation does not occur solely at the pyrrolyl-C α position and the conjugation is interrupted.

Introduction

The size, shape, (relative) stability and ease of synthesis of DNA, allied to the well-known rules for structure-building through base-pair hydrogen bonding, have led to its increased role as a material for bottom-up nanoscale fabrication.^{1–3} One of the key areas of interest here is in nanoscale electronics, where DNA is envisaged as a means of self-assembling circuitry. However, the lack of electrical conductance of natural nucleic acids⁴ has prompted efforts to introduce this property into DNA-based materials.

Towards this end, DNA is most commonly used as a template for the deposition and growth of metallic^{5–15} or semiconducting materials,^{16,17} generating so-called nanowires (Scheme 1). This generally applicable approach is synthetically expedient, can



Scheme 1 Illustration of the difference in DNA-based materials resulting from using duplex DNA as a template (top) or as a scaffold by introducing new functionality in one of the strands (bottom).

provide thin (~5 nm) structures, and allows the use of long (typically >10 μ m) DNA strands. The length of these facilitates the fabrication of simple electrical circuits using the resultant nanowires as active components.^{5,6,16,18}

An alternative approach is to use DNA as a scaffold (Scheme 1). Here the DNA, or its constituent groups, is modified in such a manner as to retain the self-assembling and structure-building capability, while introducing new functionality. Functionalisation of nucleosides¹⁹ is used widely in fields such as medicine (anticancer^{20–22} and antiviral agents^{23,24}) or biological analysis (e.g. DNA sequencing,²⁵ a range of redox- and photo-active²⁶ groups

^aChemical Nanoscience Laboratory, School of Chemistry, Newcastle University, Newcastle upon Tyne, NE1 7RU, U.K. E-mail: Andrew.houlton@ncl.ac.uk; Fax: 0044-(0)191222 6929; Tel: 0044-(0)191222 6262

^bCrystallography Laboratory, School of Chemistry, Newcastle University, Newcastle upon Tyne, NE1 7RU, U.K. Fax: 0044-(0)191222 6929; Tel: 0044-(0)191222 6641

† Electronic supplementary information (ESI) available: CV charts, Table S1, ¹H-NMR and ¹³C-NMR spectra. X-ray crystallographic data in CIF format, for 5 compounds reported herein. CCDC reference numbers 785461–785465. For ESI and crystallographic data in CIF or other electronic format see DOI: 10.1039/c0ob00466a

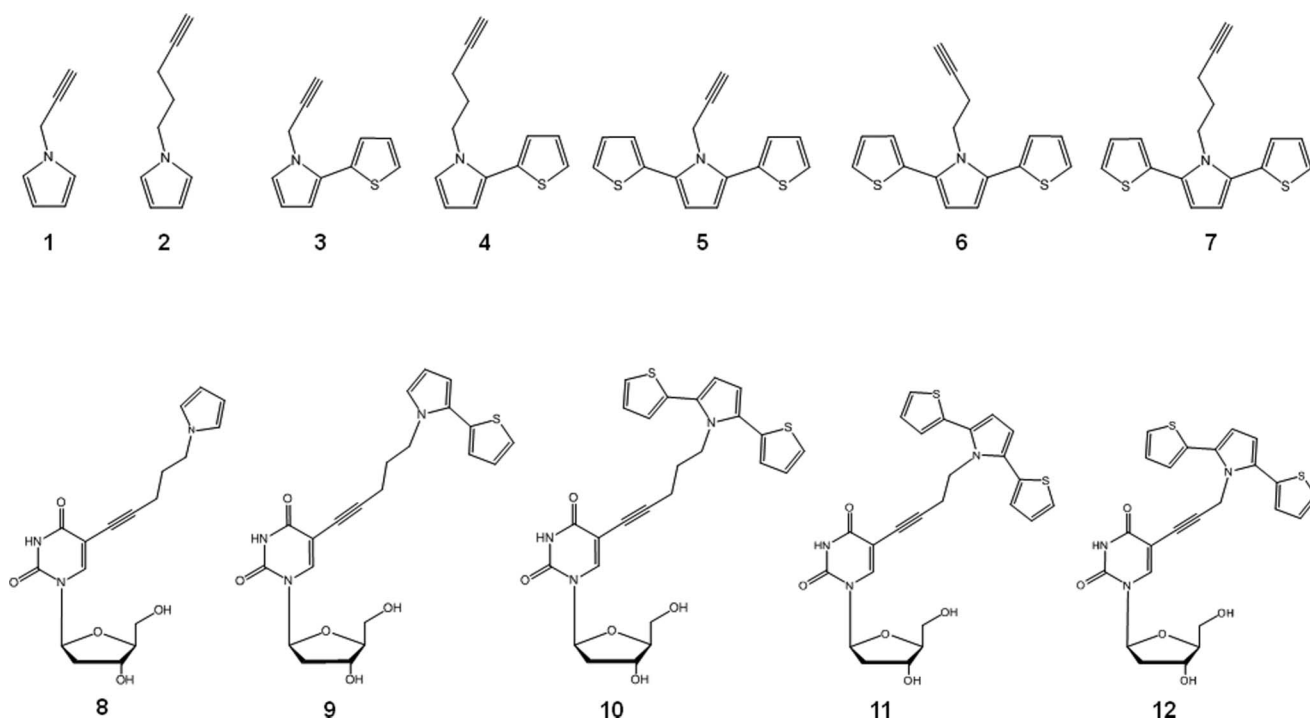


Fig. 1 Structures of *N*-alkylated alkynyl units **1–7** and modified thymidine derivatives **8–12**.

such as ferrocenyl^{27–29}), and coordination complexes^{30–32} have been also introduced for such applications.

However, this approach has only been adopted for materials-type applications relatively recently. Examples of this have been demonstrated by the replacement of natural base pairs with metal-chelating variants,^{33–36} with the resulting materials exhibiting cooperative magnetic behaviour, for example.³⁷ Other examples include the introduction of multiple adjacent porphyrin groups into short oligonucleotides forming discrete photoactive regions of defined length.^{26,38,39}

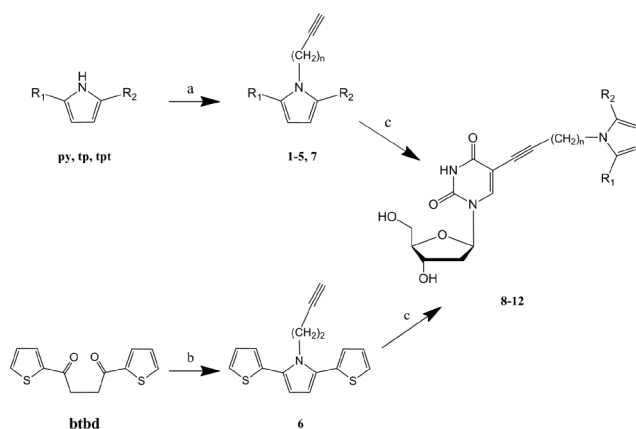
An elegant, purely organic, strategy has been described by Schuster^{40–43} where nucleosides modified with organic “monomer” units are subsequently oligomerised to give DNA conjoined with a conductive polymer. Conducting polymers of this type, such as polyaniline,^{44,45} polypyrrole,^{18,46} and polyindole,⁴⁷ have previously been grown as long (> 10 μm) nanowires using DNA-templating methods and in some cases have been shown to be electrically conducting.^{18,46–48}

We have begun to extend our work on DNA-based materials^{15,16,18,28,29,46–51} towards this DNA-as-scaffold approach. As a first step we report here the synthesis and characterisation of 5-modified thymidine nucleosides bearing pyrrolyl (**py**), 2-(2-thienyl)pyrrolyl (**tp**) and 2,5-bis(2-thienyl)pyrrolyl (**tpt**) as substituents attached *via* alkyl-alkynyl chains of 3, 4 and 5 carbon atoms in length. Each of these heterocycles is known to polymerise to give electrically conducting polymers upon oxidation.^{52,53}

Results and Discussion

Synthesis and characterisation of *N*-alkylated alkynyl units (**1–7**) and C5-modified nucleobases (**8–12**)

The target compounds **8–12**, along with the precursors **1–7**, are shown in Fig. 1. The general synthetic route for the modified



Scheme 2 Synthetic route for *N*-alkylated pyrrole derivatives **1–7** and modified nucleosides **8–12**. (a) NaH, alkynyl derivative (propargylbromide or 5-chloro-1-pentyne), DMF, rt; (b) 4-amino-1-butyne, propionic acid, toluene, reflux; (c) 5-iodo-deoxyuridine, Pd(PPh₃)₂Cl₂, CuI, Et₃N, DMF, rt. R₁ = R₂ = H (**py**); R₁ = H, R₂ = thienyl (**tp**); R₁ = R₂ = thienyl (**tpt**). *m* = 1 or 3. *n* = 1, 2 or 3.

nucleosides is shown in Scheme 2 and involves Sonogashira-type Pd-catalysed C–C coupling of 5-iodo-deoxyuridine with a terminal alkynyl group. The latter was presented as an *N*-alkyl-alkynyl chain, which provides a straightforward way to vary the separation between the nucleobase and the pyrrolyl unit as well as allowing the pyrrolyl unit to be extended in the series **py** → **tp** → **tpt**. *N*-alkylated derivatives **1–5** and **7**, with 3- or 5-carbon-atom length chains were synthesised by initial deprotonation of the **py**, **tp** or **tpt** unit with sodium hydride and subsequent alkylation using the appropriate haloalkyl-alkynyl derivative, propargylbromide or 5-chloro-1-pentyne, respectively.

Attempts to *N*-alkylate the **tpt** unit with 4-bromo-1-butyne to obtain **6** were unsuccessful. This is likely due to competitive elimination of 4-bromo-1-butyne to give but-1-en-3-yne, as the same problem was previously found for 4-bromo-1-butene.⁵⁴ Instead, the synthesis of compound **6** was performed using a Paal–Knorr condensation reaction between 4-bis(2-thienyl)butane-1,4-dione and 4-amino-1-butyne (Scheme 2).^{55,56}

All the *N*-alkylated derivatives, **1–7**, were characterised by ¹H NMR and high-resolution ES-MS spectroscopy. The ¹H NMR spectra showed the expected loss of the NH proton, along with an up-field shift for pyrrolyl protons and a down-field shift for thienyl proton resonances (compared with the corresponding unsubstituted derivatives). Further confirmation of the product identity was obtained from single-crystal X-ray diffraction studies in the cases of **5–7** (see ESI†).

The crystal structures of compounds **5** and **6** contain two independent molecules in the asymmetric unit, with bond lengths and angles lying within the expected ranges.

In the molecular structure of **5**, the three heterocyclic rings are oriented such that the hetero atoms alternate in an up-down-up arrangement (Fig. 2). Furthermore, the thienyl rings are almost coplanar (dihedral angle 12.7°) with respect to one another, but are twisted by 29.1° and 40.7° individually with respect to the pyrrolyl group.

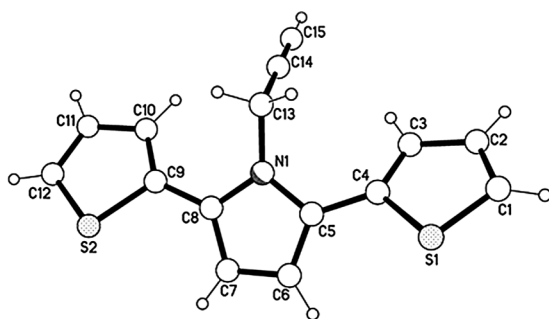


Fig. 2 View of the molecular structure of one of the independent molecules in **5**. Selected angles N1–C13–C14 115.2°, and interplanar angles; a–b 40.7°, b–c 29.1°, a–c 12.7°. Planes defined as follows: (a) S1/C1/C2/C3/C4, (b) N1/C5/C6/C7/C8, (c) S2/C9/C10/C11/C12.

The crystal structure of **6** (Fig. 3) also contains two independent molecules differing primarily with regard to the orientations of the thienyl rings, disordered over two positions. Similar disorder has been reported before in thienyl rings of **tpt**.⁵⁷

The molecular structure of compound **7** (Fig. 4), the **tpt**-derivative with a C₅ chain, reveals an up-up-down arrangement of the heteroatoms, though again there is some disorder in the thienyl S1-ring. Here the thienyl–pyrrolyl interplanar angles are slightly larger, 40.0° and 41.1°, than is seen in one of the independent molecules of **6**.

Generally, the pyrrolyl–thienyl interplanar angles found for our compounds lie within the range 29–41°, with the exception of one independent molecule found in the crystal structure of **6** with a range of 48.4–65.8°. This is consistent with the four previously reported observations on *N*-alkylated **tpt** derivatives with unmodified pyrrolyl and thienyl rings (Cambridge Structural Database, 2010 release).⁵⁸ Ferraris *et al.* reported the structure of an *N*-methyl **tpt** derivative with interplanar angles in the range

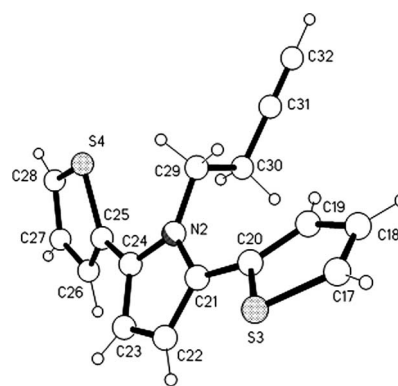


Fig. 3 View of the molecular structure of one of independent molecules in **6**. Selected angles N1–C13–C14 111.0°, N2–C29–C30 110.7° and interplanar angles a–b 48.4°, b–c 65.8°, a–c 69.2°, a'–b' 33.2°, b'–c' 31.1°, a'–c' 62.6°. Planes defined as follows: (a) S1/C1/C2/C3/C4, (b) N1/C5/C6/C7/C8, (c) S2/C9/C10/C11/C12, (a') S3/C17/C18/C19/C20, (b') N2/C21/C22/C23/C24, (c') S4/C25/C26/C27/C28.

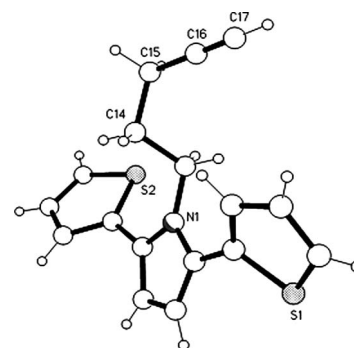
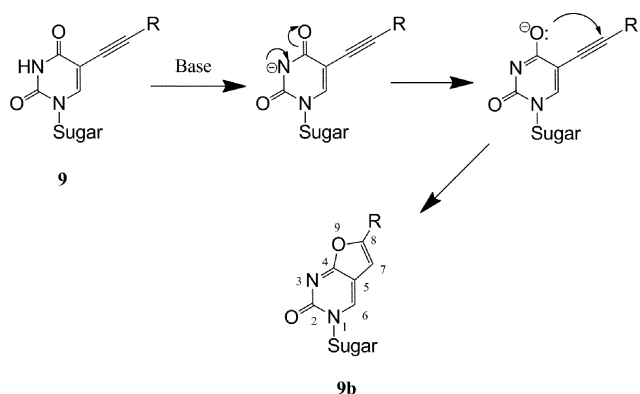


Fig. 4 Views of the molecular structure of **7**. The major component of the disordered molecule is shown. Selected angles: N1–C13–C14 112.8°, and interplanar angles: a–b 40.0°, b–c 41.1°, a–c 76.4°. Planes defined as follows: (a) S1/C1/C2/C3/C4, (b) N1/C5/C6/C7/C8, (c) S2/C9/C10/C11/C12.

31.3–34.2°.⁵⁷ In the case of two phenyl-substituted derivatives the pyrrolyl–thienyl interplanar angles were found within the ranges 37.5–57.2° and 29.3–29.5°.^{59,60} Finally, an *N*-alkylated **tpt** unit contained in a flavin-based rotaxane showed interplanar angles within the range 52.0–71.1°,⁶¹ although in this instance steric hindrance may well force such large interplanar angles.

Modified Nucleosides: Synthesis of the modified nucleosides **8–12** was carried out using Sonogashira coupling of 5-iodo-2'-deoxyuridine and the appropriate *N*-alkylated alkynyl derivative (Scheme 2). The catalytic conditions employed were a modification of those reported by Ghilagaber *et al.*,⁶² using bis(triphenylphosphine)dichloropalladium(II) (0.15 equiv) as catalyst. Typical yields varied from 30 to 78% though the yield of the pyrrolyl derivative **8** was rather less (10%). All modified nucleosides were characterised by ¹H NMR and high-resolution ES-MS spectroscopy.

In a preparation of **9** there was evidence of a second compound, **9b**, as indicated by the appearance of an uncoupled proton at $\delta = 6.37$ ppm in the ¹H NMR spectrum. This was indicative of the formation of the furanopyrimidone isomer (**9b**, Scheme 3). Other features that are supportive of this assignment are the



Scheme 3 Proposed mechanism for the formation of furanopyrimidone isomer **9b** from **9**, R = $-(\text{CH}_2)_3\text{-tp}$.

down-field shift in the H6 resonance ($\delta = 8.67$ ppm. (**9b**) cf. 8.01 ppm. (**9**)). This rearrangement of alkynyl-thymidine derivatives is known^{63–65} and we have previously observed this ourselves with C5-ferrocenylethynyl-deoxythymidine.²⁹ The proposed mechanism for rearrangement is presented in Scheme 3 and involves base-catalysed formation of the O4-alkoxide which cyclises by attack at the alkyne function.

Unequivocal confirmation of **9b** as the furanopyrimidone isomer was obtained from a single-crystal structure analysis (Fig. 5). This analysis showed that the **tp** unit lies over the furanopyrimidine ring with a shortest distance H21 \cdots O4 of 2.68 Å. The interplanar angle between the pyrrolyl and thienyl rings is 34.1° and the two rings are in an up-down arrangement, though again the thienyl ring is disordered over two positions.

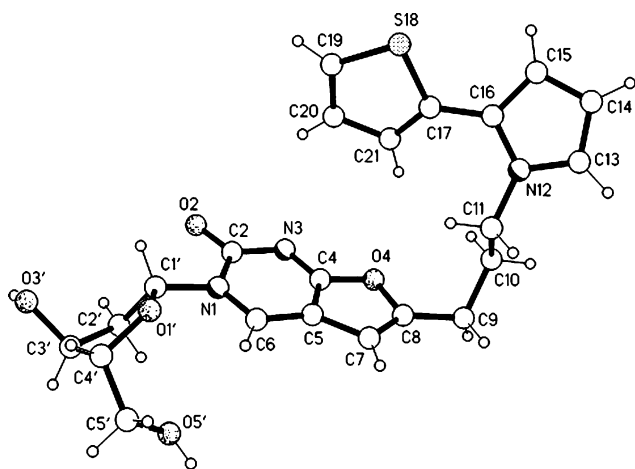


Fig. 5 Molecular structure of the furanopyrimidone derivative **9b**. Selected distances (Å): O2–C2 1.231(5), C2–N3 1.368(6), C2–N1 1.407(6), N1–C6 1.343(6), C6–C5 1.364(6), C5–C4 1.393(6), N3–C4 1.306(6), C4–O4 1.370(5), O4–C8 1.418(5), C8–C9 1.481(6), C8–C7 1.320(7), C7–C5 1.456(6).

The nucleoside exhibits an *anti* arrangement with the deoxyribose unit adopting a C2'-*endo* conformation. Hydrogen bonding involving O2 of the furanopyrimidone and H3' of the sugar (O2 \cdots H3' = 1.92 Å; generated by the symmetry operator $-x + 1, 0.5 + y, -z + 2$) is seen between the molecules, forming extended C(8) chains⁶⁶ running through the crystal structure.

Table 1 Wavelengths of maximum absorption (λ_{max}) and molar extinction coefficients (ϵ) for modified nucleosides **8–12**

Compound	λ_{max} (nm)	ϵ ($\text{M}^{-1}\text{cm}^{-1}$)
8	289	8.12×10^3
9	291	1.22×10^4
10	306	1.31×10^4
11	297	2.06×10^4
12	297	2.11×10^4

Electronic structure: UV–vis spectroscopy

UV–visible spectroscopy (UV–vis) was used to study the electronic structure of the modified nucleosides **8–12** (Fig. 6). Table 1 presents the wavelengths of maximum absorption (λ_{max}) and the molar extinction coefficients (ϵ).

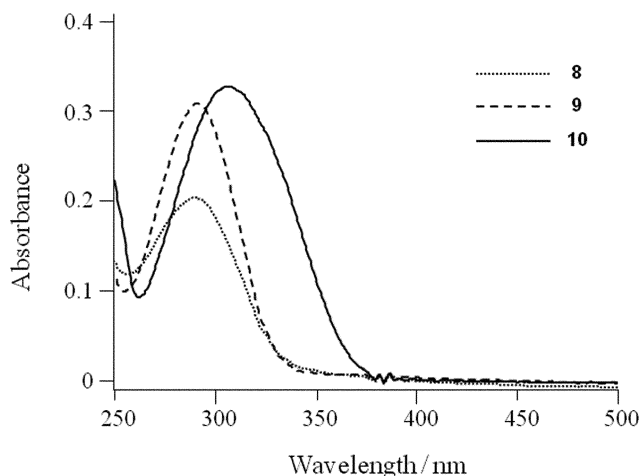


Fig. 6 UV–vis spectra for compounds **8–10**. All spectra were recorded at 0.025 mM of the title compounds in MeOH.

For the series of compounds containing a pentynyl bridge, **8–10**, the expected red-shift is observed as the aromatic group increases in size in the order **py** < **tp** < **tpt**, although this is small in the case of **8** > **9**. This trend is also apparent in the decreasing separation between the HOMO and LUMO energies derived from DFT calculations (see later).

Inspection of these orbitals also indicates that, in all cases, the transition is dominated by electronic excitation from an orbital largely based on the pyrrolyl-containing aromatic unit to one on the nucleobase. The effect of increasing alkyl-chain length for the **tpt** derivatives, **10–12**, does not show any notable trend. The DFT calculations indicate that the HOMO–LUMO transition involves similar electronic excitation.

Electrochemistry

The redox behaviour of the compounds was investigated using cyclic voltammetry (CV) and the data are summarised in Table 2. In some cases no clear oxidation peak is observed, therefore we have also tabulated the potential at a fixed anodic current of 0.1 mA. The CVs of the *N*-alkyl-alkynyls **2**, **4** and **7** bearing the same 5-carbon alkyl chain linked to **py**, **tp** or **tpt** respectively are shown in Figures S4–S8 (see ESI†). The anodic peak (E) is less positive for the more extended ring systems in the order **2** > **4** > **7**, (>1.5, 1.04, 0.986 V) in agreement with the trend followed by

Table 2 CV oxidation peaks of monomer units and alkylated monomer units obtained from the cyclic voltammograms. Conditions: 10 mM of sample, 100 mM LiClO₄, acetonitrile, r.t., working electrode Pt, counter electrode Au and Ag quasi-reference electrode. Scan rate 0.2 V s⁻¹

Compound	E/V (peak)	E/V (I = 0.1 mA)
py	> 1.50	1.05
tp	1.15	1.03
tpt	1.07	0.89
2	> 1.5	1.08
4	1.04	0.89
5	1.30	1.17
6	0.98	0.85
7	0.99	0.78
8	1.37	—
9	> 1.50	1.26
10	1.33	0.95
11	1.16	1.16
12	1.42	1.14

the sequence of peak potentials for the free monomer units **py** > **tp** > **tpt** (>1.5, 1.15, 1.07 V) (Table 2 and ESI†). However, for **tpt** derivatives **5**, **6** and **7**, the oxidation potential variation shows no particular trend (1.30, 0.98, 0.99 V) with increasing chain length. The CVs for modified nucleosides (Fig. 7) show small changes for the oxidation potential between compounds **10**, **11** and **12** bearing the **tpt**.

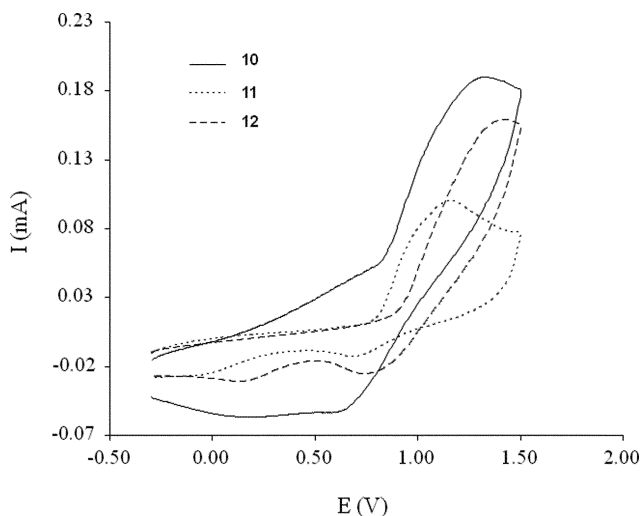


Fig. 7 CVs for compounds **10**, **11**, **12** comparing the effect of different bridge length, (CH₂)₃, (CH₂)₂ and (CH₂) respectively, linking the **tpt** to the nucleoside. Conditions: 10 mM of sample, 100 mM LiClO₄, acetonitrile, r.t., working electrode Pt, counter electrode Au and Ag quasi-reference electrode. Scan rate 0.2 V s⁻¹.

The results for these compounds show that the anodic peak oxidation potential of the **tpt** unit linked to the nucleoside is not strongly affected by the choice of carbon-bridge and, as for the corresponding *N*-alkylated monomers, no particular trend is observed; compound **11** has the lowest oxidation potential.

In contrast, when comparing the different substituent units, **py**, **tp** and **tpt**, linked to the nucleoside by the same 5-carbon bridge, significant changes appear in the cyclic voltammograms (Fig. 8, and ESI†). Compounds **9** and **10** show clear evidence of conductive polymer formation (broad reduction peak centred near 0.2 V). However, the **py**-based compound **8** produces a poorly

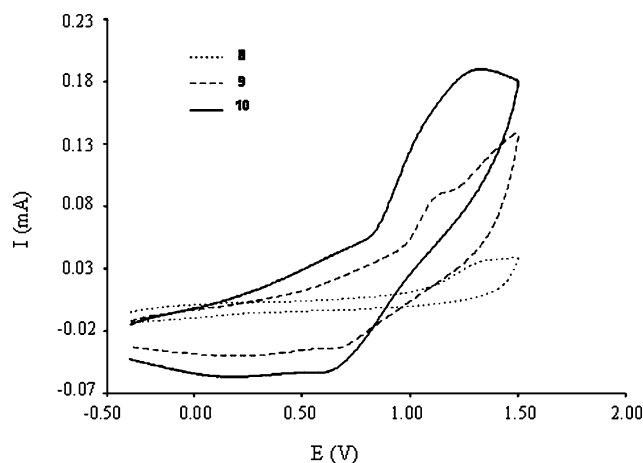


Fig. 8 CVs for compounds **8**, **9** and **10** comparing the effect of different substituent units (**py**, **tp** and **tpt** respectively) linked to the nucleoside by a 5-carbon bridge. Conditions: 10 mM of sample, 100 mM LiClO₄, acetonitrile, r.t., working electrode Pt, counter electrode Au and Ag quasi-reference electrode. Scan rate 0.2 V s⁻¹.

conductive film as evident in the low currents observed and the lack of well-defined surface waves. This is typical for a poorly conductive polymer that insulates the electrode.

Electronic structure calculations

To gain further insight into the electronic structure of the modified nucleosides, particularly the effects of oxidation, a series of geometries were optimised by DFT calculations using the B3LYP functional and the 6-31G(*) basis set. The calculations were performed on compounds **8–12** and related derivatives in the series (see Fig. 9 and Table 3). Equilibrium geometries were obtained for both the neutral molecule and the corresponding one-electron-oxidised cation in each case. Comparison of the equilibrium geometries for the neutral molecules with the structures derived from X-ray diffraction reveals essentially similar features. For example, bond lengths and angles are in the normal range and in all cases the deoxyribose ring adopts a *C2'-endo* conformation as seen in the X-ray structure of **9b**. A point of difference is that the nucleoside adopts a *syn*-conformation rather than the *anti*-conformation seen in **9b**. This is due to the formation of an intramolecular hydrogen bond between the C5'-OH and the O2 carbonyl group of the thymidine. The same intramolecular hydrogen bond was found during a DFT study of 2'-deoxycytidine, leading to a more stabilised *syn*-orientation of the base unit with respect to the sugar unit.⁶⁷

The E_{HOMO} energy is raised as the size of the nucleoside substituent group increases, **py** < **tp** < **tpt**, and is in keeping with the electrochemical data (*vide infra*).

Table 3 Calculated energies (eV) for the modified nucleosides, **8–12**

Compound	E _{HOMO} (eV)	E _{LUMO} (eV)	E _{HOMO-LUMO} gap
8	-5.57	-1.52	-4.05
9	-5.37	-1.48	-3.89
10	-5.19	-1.43	-3.76
11	-5.15	-1.52	-3.63
12	-5.21	-1.49	-3.72

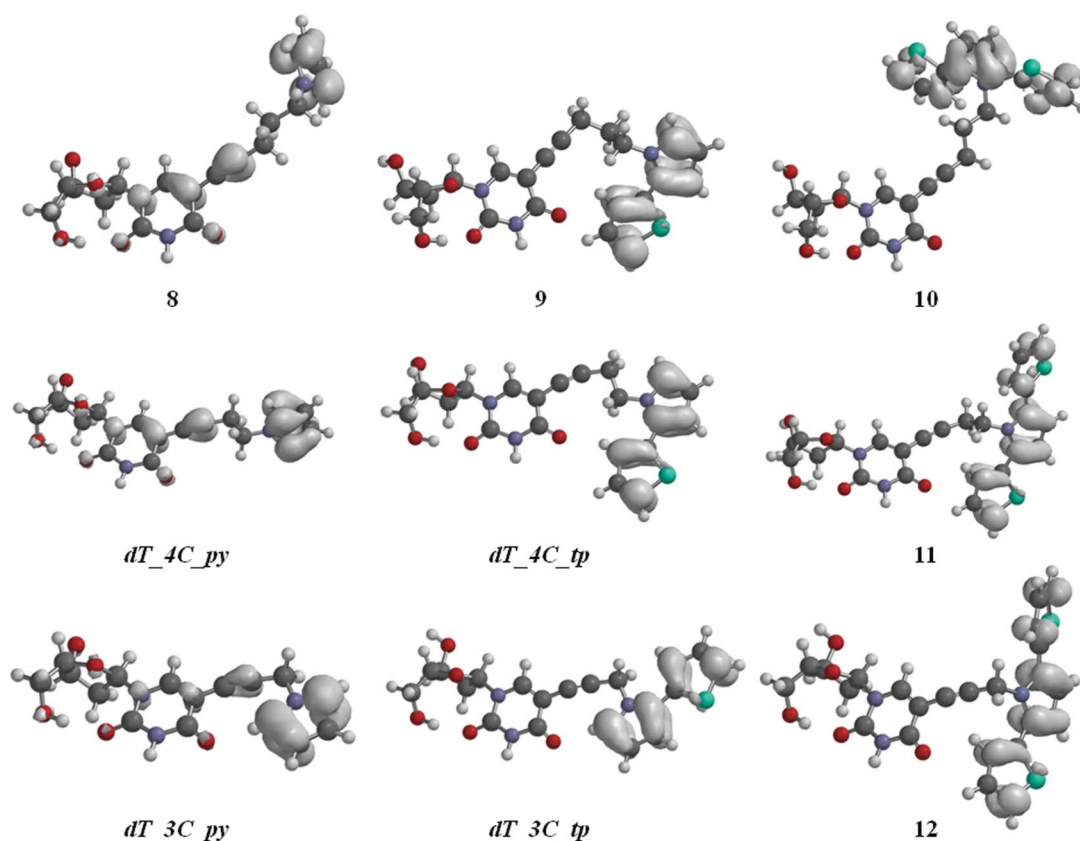


Fig. 9 DFT-calculated spin density distribution on modified nucleosides **8–12** and analogues, bearing the monomer units **py**, **tp** or **tpt** linked through a 5- 4- or 3-carbon bridge to the nucleoside.

The $E_{\text{HOMO}}-E_{\text{LUMO}}$ gap decreases in the same order, as expected, in agreement with the electronic absorption spectroscopy studies (Table 3).

For the one-electron oxidised cations, the calculated spin density serves extremely well to illustrate the extent of delocalisation over the molecules (Fig. 9). An NAPC (Natural Atomic Populations and Charges) analysis is shown in Table 4 as a quantitative guide. For this, the molecule is considered as comprising four components: substituent unit/bridge/nucleobase/sugar. As can be seen, for all types of substituent, the majority of the spin density resides on this unit, **py**, **tp** or **tpt**, respectively. However, further inspection reveals that the **py** series is distinct in that there is much greater transfer of spin over the whole molecule, almost 50% in two cases, compared to the **tp** or **tpt** derivatives. A simple explanation for this can be based on a consideration of the size, and therefore extent of conjugation, in the substituent unit, which increases in the order **py** < **tp** < **tpt**.

A somewhat unexpected finding in the **py** series is that the largest delocalisation of spin density (~47%) is observed for compound **8**, a derivative with the longest alkyl chain, $(\text{CH}_2)_3$.

An increase in spin density is seen on both the bridging unit ($6.6 < 15.4 < 17.6\%$) and the deoxythymidine group ($9.7 < 22.9 < 25.6\%$) as alkyl chain length is increased, $-(\text{CH}_2)-$; $-(\text{CH}_2)_2-$; $-(\text{CH}_2)_3-$ (Table 4).

A simple rationalisation of this phenomenon is not obvious.⁶⁸ Interestingly, these results, of spin density distributed over the different parts of the molecules, suggest that the polymerisation would take place through different positions giving rise to an

Table 4 NAPC analysis of spin density on the modified nucleosides **8–12** and analogues

Derivative	Substituent (pyrrolyl/thienyl) ^a	Bridge ^b	Nucleobase ^c	Sugar ^d
8	52.6	17.6	25.6	4.3
<i>dT_4C_py</i>	56.2	15.4	22.9	5.5
<i>dT_3C_py</i>	79.8	6.6	9.7	4.0
9	100 (55.5/44.5)	0	< 0.1	0
<i>dT_4C_tp</i>	100 (56.9/43.1)	0	< 0.1	0
<i>dT_3C_tp</i>	99.4 (60.9/38.5)	0.2	0.4	< 0.1
10	99.9 (48.5/51.4)	< 0.1	< 0.1	0
11	100 (47.8/52.2)	0	0	0
12	100 (48.6/51.4)	0	0	0

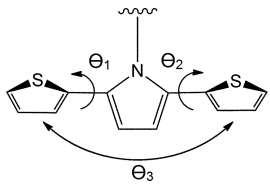
^a Total percentage on substituent unit. The distribution across the pyrrolyl and thienyl rings is shown in brackets where appropriate. ^b Percentage on alkyl chain bridge. ^c Percentage on the thymidine nucleobase. ^d Percentage on the sugar unit.

irregular polymer and therefore will make this compound less suitable for the synthesis of conducting polymers. This is again in agreement with the CV data.

In the **tp**- or **tpt**-containing series, spin density is almost wholly located (>99%) on the thienyl-pyrrolyl unit. This is found irrespective of the length of the carbon bridge and is consistent with the increased size of the aromatic unit.

It was of interest to compare the structures of the neutral parent compounds with the oxidised species for these two series of compounds. It is known that the inter-ring torsion angle (θ) affects

Table 5 DFT-calculated angles between planes defined by pyrrolyl and thienyl rings for both neutral and cationic modified nucleobases



Derivative	TP (θ_1)	TP* (θ_1)	TPT($\theta_1/\theta_2/\theta_3$)	TPT* ($\theta_1/\theta_2/\theta_3$)
9	47.5°	7.8°		
<i>dT_4C_tp</i>	47.8°	1.2°		
<i>dT_3C_tp</i>	50.0°	0.7°		
10			45.5°/45.3°/24.1°	28.7°/14.8°/13.9°
11			45.0°/44.9°/24.0°	31.3°/2.0°/31.9°
12			44.9°/43.7°/25.0°	32.7°/15.3°/47.7°

the intrinsic bandgap of isolated conjugated polymer chains and consequently the conductivity along its length.⁵³ Table 5 presents the inter-ring torsion angles between the pyrrolyl and thienyl rings in each case. For the **tp** series the torsion angle, θ_1 , between pyrrolyl and thienyl rings decreases by at least 40° as a consequence of oxidation. For the **tpt** series the equivalent torsion angles, θ_1 and θ_2 , decrease in all cases, and there is a slight increase in the torsion angles between the thienyl rings (θ_3) for compounds with longer carbon bridges (Table 5). Overall, though, the effect of oxidation is to increase conjugation as indicated by a shortening of the C–C bond(s) linking the pyrrolyl and thienyl rings (Table S1, see ESI†) and an increase in the coplanarity of the group.

It is worth noting that the reported decrease in conductivity of *N*-substituted polypyrrole-type polymers, compared to the unsubstituted parent system, has been ascribed as being primarily due to steric hindrance inhibiting adoption of a coplanar geometry.⁵⁷

In order to maintain a high electrical conductivity, in polypyrrole and polythiophene, the angles between the rings should be below 40°. ⁶⁹ The DFT calculations here show that the presence of the attached nucleoside does not significantly hinder this process upon oxidation. Therefore it is expected that the electrical conductivity of polymers formed from these systems will not be extensively affected by steric interferences.

Conclusions

We have prepared a series of modified nucleosides bearing substituent groups that can be electrochemically polymerised. The more extended 2-(2-thienyl)pyrrolyl- and 2,5-bis(2-thienyl)pyrrolyl- systems have lower anodic peak potentials, E_p , and yield conducting polymer films upon oxidation. Both of these systems appear to be well suited for the development of conducting DNA-based materials and such studies are ongoing.

Experimental Section

Materials. Reagents were purchased from Aldrich and used as received unless otherwise stated. Pyrrole (**py**) was distilled prior to use. 1,4-Bis(2-thienyl)butane-1,4-dione (**btbd**),⁷⁰ 2-(2-thienyl)pyrrole⁷¹ (**tp**), 4-amino-1-butyne (Figure S14, ESI†)^{72,73} and *N*-(prop-2-ynyl)pyrrole (**1**)⁷⁴ were synthesised according to the literature methods. Triethylamine was distilled from KOH and

then degassed with dry N₂ for 30 min. Anhydrous DMF was used as received and degassed with dry N₂ for 30 min. All reactions were performed under N₂ using standard Schlenk techniques. NMR experiments were performed on a 300 MHz Bruker Spectrospin WM 300 WB spectrometer, electronic absorption spectra were recorded on a Hitachi U-3010 Spectrophotometer, infrared spectra were recorded on a Varian 800 FT-IR (Scimitar Series) spectrometer and high resolution mass spectra with electrospray ionization (HRMS-ESI) were measured on a Waters Micromass LCT Premier mass spectrometer.

General procedure for the alkylation of 2-(2-thienyl)pyrrole and 2,5-bis(2-thienyl)pyrrole (2–5, 7). The appropriate monomer unit (5 mmol) was dissolved in anhydrous DMF (100 mL). To this solution sodium hydride (60% dispersion in mineral oil) (1.5 equiv) was added under nitrogen and the mixture was stirred until H₂ evolution ceased. The appropriate alkynyl derivative (2 equiv) was then added and the mixture was stirred in the dark overnight. The resulting suspension was filtered through Celite and the solvent removed *in vacuo*. Water (100 mL) was added and the resulting mixture was extracted with CH₂Cl₂ (3 × 200 mL) and the solution dried over magnesium sulfate. The solvent was removed *in vacuo* and the crude product was purified on silica using a gradient of 0–5% ethyl acetate in hexane. The appropriate fractions were combined and solvent was removed *in vacuo* to yield the pure product.

***N*-(Pent-4-ynyl)pyrrole (2).** Yield: 80% as an oil. ¹H NMR (CDCl₃): δ = 1.96 (m, 2H, CH₂), 2.03 (t, 1H, CH), 2.16 (m, 2H, CH₂), 4.05 (t, 2H, CH₂), 6.16 (t, 2H, CH_{py}), 6.68 (t, 2H, CH_{py}). ¹³C-NMR (CDCl₃): δ = 120.70, 108.45, 83.10, 69.68, 47.92, 30.38, 15.75. IR (neat, cm⁻¹): 3295, 2120, 1500, 1282, 1089, 722. HRMS (ESI): *m/z*: calc for C₉H₁₁N [M+H]⁺: 134.0958; found: 134.0970.

***N*-(Prop-2-ynyl)-2-(2-thienyl)pyrrole (3).** Yield: 8% as an oil. ¹H NMR (CDCl₃): δ = 2.42 (t, 1H; CH), 4.75 (d, 2H; CH₂), 6.24 (t, 1H; CH_{py}), 6.33 (q, 1H; CH_{py}), 6.94 (q, 1H, CH_{py}), 7.08 (m, 1H, CH_{th}), 7.13 (dd, 1H, CH_{th}), 7.32 (dd, 1H, CH_{th}). ¹³C-NMR (CDCl₃): δ = 134.60, 127.68, 126.93, 126.20, 125.57, 122.86, 111.24, 109.23, 79.09, 73.72, 37.17. IR (neat, cm⁻¹): 3287, 2121, 1291, 843, 788, 695. HRMS (ESI): *m/z*: calc for C₁₁H₉NS [M+H]⁺: 188.0531; found: 180.0534. UV (MeOH): λ_{\max} 290 nm

***N*-(Pent-4-ynyl)-2-(2-thienyl)pyrrole (4).** Yield: 70% as an oil. ¹H NMR (CDCl₃): δ = 1.92 (m, 2H, CH₂), 2.03 (t, 1H, CH), 2.19 (m, 2H, CH₂), 4.19 (t, 2H, CH₂), 6.23 (m, 1H, CH_{py}), 6.36 (m, 1H, CH_{py}), 6.84 (s, 1H, CH_{py}), 7.08 (m, 2H, CH_{th}), 7.31 (m, 1H, CH_{th}). ¹³C-NMR (CDCl₃): δ = 135.33, 127.51, 126.73, 125.93, 125.21, 123.37, 111.19, 108.49, 83.26, 69.62, 46.43, 30.36, 16.08. IR (neat, cm⁻¹): 3290, 2130, 1429, 1298, 843, 787, 695. HRMS (ESI): *m/z*: calc for C₁₃H₁₃NS [M+H]⁺: 216.0843; found: 216.0847. UV (MeOH): λ_{\max} 284 nm.

***N*-(Prop-2-ynyl)-2,5-bis(2-thienyl)pyrrole (5).** Yield: 69% as a solid, mp 121–122 °C. ¹H NMR (CDCl₃): δ = 2.52 (t, 1H, CH), 4.77 (d, 2H, CH₂), 6.40 (s, 2H, CH_{py}), 7.13 (m, 2H, CH_{th}), 7.32 (dd, 2H, CH_{th}), 7.40 (m, 2H, CH_{th}). ¹³C-NMR (CDCl₃): δ = 134.82, 129.26, 127.87, 126.12, 125.70, 111.23, 80.74, 73.71, 35.90. IR (neat, cm⁻¹): 3263, 2119, 1494, 1422, 1333, 1200, 844, 772, 695. HRMS (ESI): *m/z*: calc for C₁₅H₁₁NS₂ [M+H]⁺: 270.0394; found: 270.0411. UV (MeOH): λ_{\max} 318 nm. Single crystals of **5** suitable

for X-ray diffraction were obtained by concentration of a solution in ethyl acetate.

***N*-(Pent-4-ynyl)-2,5-bis(2-thienyl)pyrrole (7).** Yield: 46% as a solid, mp 36–40 °C. ¹H NMR (CDCl₃): δ = 1.78 (m, 2H, CH₂), 1.86 (t, 1H, CH), 2.03 (m, 2H, CH₂), 4.28 (m, 2H, CH₂), 6.36 (s, 2H, CH_{py}), 7.11 (m, 4H, CH_{th}), 7.33 (m, 2H, CH_{th}). ¹³C-NMR (CDCl₃): δ = 135.30, 128.84, 127.58, 126.51, 125.65, 111.53, 83.05, 69.22, 44.61, 30.12, 16.12. IR (neat, cm⁻¹): 3279, 2120, 1470, 1410, 1305, 1198, 837, 754, 696. HRMS (ESI): *m/z*: calc for C₁₇H₁₅NS₂ [M+H]⁺: 298.0724; found: 298.0718. UV (MeOH): λ_{max} 309 nm. Single crystals of **7** suitable for X-ray diffraction were obtained by concentration of a solution in ethyl acetate.

Synthesis of *N*-(but-3-ynyl)-2,5-bis(2-thienyl)pyrrole (6). A solution of 1,4-bis(2-thienyl)butane-1,4-dione (6 g, 14.5 mmol), 4-amino-1-butyne (1 g, 14.5 mmol), propionic acid (2 mL, 27 mmol) in anhydrous toluene (100 mL) was refluxed with molecular sieves 4 Å (2 g) under nitrogen. After 20 h, additional molecular sieves 4 Å (2 g) were added, and the mixture was refluxed for a total of 70 h. The reaction mixture was concentrated *in vacuo* and the residue dissolved in ethyl acetate (150 mL). This was washed with aqueous sodium bicarbonate (2 × 100 mL), and aqueous sodium chloride (100 mL) and then dried over magnesium sulfate. After filtration the solvent was removed and the crude product was purified on silica using hexane–ethyl acetate (95 : 5) as eluent. This afforded **6** in 37% yield (1.5 g) as a solid, mp 60–62 °C. ¹H NMR (CDCl₃): δ = 1.86 (t, 2H, CH), 1.86 (t, 1H, CH), 2.34 (m, 2H, CH₂), 4.26 (m, 2H, CH₂), 6.27 (s, 2H, CH_{py}), 7.02 (m, 4H, CH_{th}), 7.26 (m, 2H, CH_{th}). ¹³C-NMR (CDCl₃): δ = 134.95, 128.65, 127.68, 126.60, 125.88, 111.72, 80.51, 70.60, 44.06, 21.16. IR (neat, cm⁻¹): 3250, 2125, 1458, 1401, 1305, 1195, 846, 767, 692. HRMS (ESI): *m/z*: calc for C₁₆H₁₃NS₂ [M]⁺: 283.0490; found: 283.0494. UV (MeOH): λ_{max} 309 nm. Single crystals of **6** suitable for X-ray diffraction were obtained by concentration of a solution in ethyl acetate.

General procedure for C5-modified nucleoside synthesis (8–12). A Schlenk flask was charged with 5-iodo-2'-deoxyuridine (1.0 mmol, 1 equiv) and made up to a 0.13 M solution in anhydrous degassed DMF. To this were added bis(triphenylphosphine)dichloropalladium(II) (0.15 mmol, 0.15 equiv), copper(I) iodide (0.2 mmol, 0.2 equiv), anhydrous degassed triethylamine (2.0 mmol, 2 equiv) and the appropriate alkynyl derivative (1.5 mmol, 1.2 equiv). The reaction mixture was stirred at room temperature for ~15 h during which time product formation was monitored by TLC. A 5% (v/w) aqueous solution of Na₂-EDTA (5 mL) was added to quench the reaction and solution was evaporated to dryness. The reaction mixture was redissolved in CH₂Cl₂ (150 mL), washed with Na₂-EDTA solution (2 × 50 mL; 5% (v/w)), water (50 mL) and then dried over sodium sulfate. After filtration and concentration *in vacuo* the crude product was loaded onto a silica column packed with CH₂Cl₂, and eluted using a gradient of 0–5% MeOH in CH₂Cl₂. Fractions containing the product were combined and the solvent was removed to yield the following compounds.

8. Yield: 10% as a off white solid, mp 65–70 °C. ¹H NMR (DMSO-d₆): δ = 1.89 (quin, 2H; CH₂), 2.12 (dd, 2H; C₂H), 2.25 (t, 2H; CH₂), 3.59 (m, 2H; C₅H), 3.79 (q, 1H; C₄H), 4.00 (t, 2H; CH₂), 4.23 (quin, 1H; C₃H), 5.13 (t, 1H; OH), 5.25 (d, 1H; OH), 5.98 (t, 2H; CH_{py}), 6.11 (t, 1H; C₁H), 6.77 (t, 2H; CH_{py}),

8.18 (s, 1H; C₆H), 11.60 (s, 1H; NH). ¹³C-NMR (dmsO-d₆): δ = 162.07, 149.82, 143.00, 120.91, 107.92, 99.29, 92.40, 88.06, 85.16, 74.11, 70.56, 61.47, 47.68, 30.40, 16.47. IR (neat, cm⁻¹): 1675, 1277, 1089, 1050, 727. HRMS (ESI): *m/z*: calc for C₁₈H₂₁N₃O₅ [M+Na]⁺: 382.1379; found: 382.1371. UV (MeOH): λ_{max} 289 nm.

9. Yield: 78% as a pale yellow solid, mp 67–70 °C. ¹H NMR (DMSO-d₆): δ = 1.80 (m, 2H; CH₂), 2.12 (dd, 2H; C₂H), 2.28 (t, 2H; CH₂), 3.58 (m, 2H; C₅H), 3.79 (q, 1H; C₄H), 4.16 (t, 2H; CH₂), 4.24 (quin, 1H; C₃H), 5.11 (t, 1H; OH), 5.25 (d, 1H; OH), 6.07 (t, 1H; CH_{py}), 6.12 (t, 1H; C₁H), 6.21 (dd, 1H; CH_{py}), 6.95 (t, 1H; CH_{py}), 7.06 (dd, 1H; CH_{py}), 7.13 (dd, 1H; CH_{py}), 7.45 (dd, 1H; CH_{py}), 8.01 (s, 1H; C₆H), 11.60 (s, 1H; NH). ¹³C-NMR (DMSO-d₆): δ = 162.03, 149.82, 143.02, 134.75, 128.05, 125.98, 125.26, 125.24, 124.10, 110.44, 108.10, 99.25, 92.29, 88.06, 85.18, 74.14, 70.61, 61.50, 46.14, 30.12, 16.49. IR (neat, cm⁻¹): 1674, 1277, 1053, 843, 696. HRMS (ESI): *m/z*: calc for C₂₂H₂₃N₃O₅S [M+Na]⁺: 464.1256; found: 464.1254. UV (MeOH): λ_{max} 291 nm.

9b. During the purification of **9**, chromatography with (9 : 1) CH₂Cl₂–MeOH showed a second product with a greater R_f. This fraction was collected and slow evaporation of the solvent gave single crystals which were analysed by X-ray diffraction and found to be of **9b**. ¹H NMR (DMSO-d₆): δ = 1.80 (m, 2H; CH₂), 2.12 (dd, 2H; C₂H), 2.28 (t, 2H; CH₂), 3.58 (m, 2H; C₅H), 3.79 (q, 1H; C₄H), 4.16 (t, 2H; CH₂), 4.24 (quin, 1H; C₃H), 5.11 (t, 1H; OH), 5.25 (d, 1H; OH), 6.07 (t, 1H; CH_{py}), 6.12 (t, 1H; C₁H), 6.21 (dd, 1H; CH_{py}), 6.37 (s, 1H; C₇H), 6.95 (t, 1H; CH_{py}), 7.06 (dd, 1H; CH_{py}), 7.13 (dd, 1H; CH_{py}), 7.45 (dd, 1H; CH_{py}), 8.67 (s, 1H; C₆H).

10. Yield: 30% as a pale yellow solid, mp 139–141 °C. ¹H NMR (DMSO-d₆): δ = 1.66 (m, 2H; CH₂), 2.12 (dd, 2H; C₂H) 2.21 (t, 2H; CH₂), 3.58 (m, 2H; C₅H) 3.81 (q, 1H; C₄H), 4.23 (m, 1H; C₃H), 4.30 (t, 2H; CH₂), 5.10 (t, 1H; OH), 5.27 (d, 1H; OH), 6.31 (t, 1H; C₁H), 6.30 (s, 2H; CH_{tpi}), 7.10 (dd, 2H; CH_{tpi}), 7.23 (dd, 2H; CH_{tpi}), 7.53 (dd, 2H; CH_{tpi}), 8.09 (s, 1H; C₆H), 11.59 (s, 1H; NH). ¹³C-NMR (DMSO-d₆): δ = 161.88, 149.80, 143.03, 134.35, 128.46, 128.15, 126.22, 126.06, 111.01, 99.23, 91.87, 88.05, 85.15, 73.92, 70.68, 61.55, 44.22, 29.87, 16.52. IR (neat, cm⁻¹): 1645, 1275, 1099, 1052, 841, 766, 692. HRMS (ESI): *m/z*: calc for C₂₆H₂₅N₃O₅S₂ [M+Na]⁺: 546.1133; found: 546.1136. UV (MeOH): λ_{max} 306 nm.

11. Yield: 35% as a pale yellow solid, mp 93–97 °C. ¹H NMR (DMSO-d₆): δ = 2.08 (dd, 2H; C₂H), 2.55 (t, 2H; CH₂) 3.56 (dd, 2H; C₅H), 3.76 (q, 1H; C₄H), 4.20 (quin, 1H; C₃H), 4.33 (t, 2H; CH₂), 5.05 (t, 1H; OH), 5.25 (d, 1H; OH), 6.08 (t, 1H; C₁H), 6.32 (s, 2H; CH_{tpi}), 7.17 (dd, 2H; CH_{tpi}), 7.27 (dd, 2H; CH_{tpi}), 7.60 (dd, 2H; CH_{tpi}), 8.25 (s, 1H; C₆H), 11.66 (s, 1H; NH). ¹³C-NMR (DMSO-d₆): δ = 161.75, 149.75, 143.47, 134.16, 128.34, 128.20, 126.66, 126.48, 111.31, 98.86, 89.05, 88.02, 85.13, 75.12, 70.63, 61.60, 43.68, 41.77, 21.61. IR (neat, cm⁻¹): 1674, 1276, 1092, 1053, 842, 769, 693. HRMS (ESI): *m/z*: calc for C₂₅H₂₃N₃O₅S₂ [M+H]⁺: 510.1158; found: 510.1185. UV (MeOH): λ_{max} 297 nm.

12. Yield: 60% as a pale yellow solid, mp 98–101 °C. ¹H NMR (DMSO-d₆): δ = 2.15 (m, 2H; C₂H), 3.60 (m, 2H; C₅H), 3.81 (q, 1H; C₄H), 4.25 (quin, 1H; C₃H), 4.92 (s, 2H; CH₂), 5.14 (t, 2H; OH), 5.28 (d, 2H; OH), 6.01 (t, 1H; C₁H), 6.34 (s, 2H; CH_{tpi}), 7.18 (dd, 2H; CH_{tpi}), 7.48 (dd, 2H; CH_{tpi}), 7.57 (dd, 2H; CH_{tpi}),

8.27 (s, 1H; C_6H), 11.69 (s, 1H; NH). ^{13}C -NMR (DMSO- d_6): δ = 161.78, 149.74, 144.40, 134.02, 128.88, 128.38, 126.26, 126.01, 110.60, 97.87, 89.28, 88.23, 85.54, 78.15, 70.56, 61.54, 48.95, 36.71. IR (neat, cm^{-1}): 1682, 1281, 1089, 1051, 843, 770, 697. HRMS (ESI): m/z : calc for $C_{24}H_{21}N_3O_5S_2$ $[M+Na]^+$: 518.0820; found: 518.0807. UV (MeOH): λ_{max} 297 nm.

X-ray crystallography. Diffraction data for **5**, **6**, **7**, **9b**, and the starting material 4-amino-1-butyne hydrochloride were measured on Nonius KappaCCD and Oxford Diffraction Gemini A Ultra diffractometers using Mo ($\lambda = 0.71073 \text{ \AA}$) and Cu ($\lambda = 1.54184 \text{ \AA}$) $K\alpha$ radiation at 150 K. The structures were solved by direct methods and refined on all unique F^2 values with anisotropic displacement parameters for non-H atoms and with a mixture of appropriately constrained, restrained and freely refined isotropic H atoms. Twofold ring-flip disorder was satisfactorily resolved and modelled for some of the thienyl rings. Full details are in the ESI,† available in CIF format.

Electronic structure calculations. All calculations were performed by using the Spartan'04 program package (Wavefunction Inc., USA) running on a Dell Optiplex 755 workstation. Molecules' geometries were optimised in DFT by using the B3LYP functional and the 6-31G(d) basis set.

Electrochemistry. Cyclic voltammograms of dissolved monomers were collected on a CH Instrument Inc. electrochemical workstation 760B (using CHI Version 5.21 software). A platinum working electrode, gold counter electrode and silver quasi-reference electrode were used. All data were collected at room temperature using acetonitrile as solvent, with 10 mM of the compound under investigation and 100 mM $LiClO_4$ as electrolyte.

Acknowledgements

We thank ONE, FP7-Marie Curie IEF (MAG) and EPSRC for funding.

Notes and references

- 1 N. C. Seeman, *Nature*, 2003, **421**, 427–431.
- 2 U. Feldkamp and C. M. Niemeyer, *Angew. Chem., Int. Ed.*, 2006, **45**, 1856–1876.
- 3 H. Li, J. D. Carter and T. H. LaBean, *Mater. Today*, 2009, **12**, 24–32.
- 4 D. Porath, A. Bezryadin, S. de Vries and C. Dekker, *Nature*, 2000, **403**, 635–638.
- 5 E. Braun, Y. Eichen, U. Sivan and G. Ben-Yoseph, *Nature*, 1998, **391**, 775–778.
- 6 E. Braun and K. Keren, *Adv. Phys.*, 2004, **53**, 441–496.
- 7 J. Richter, M. Mertig, W. Pompe, I. Monch and H. K. Schackert, *Appl. Phys. Lett.*, 2001, **78**, 536–538.
- 8 J. Richter, R. Seidel, R. Kirsch, M. Mertig, W. Pompe, J. Plaschke and H. K. Schackert, *Adv. Mater.*, 2000, **12**, 507–510.
- 9 W. E. Ford, O. Harnack, A. Yasuda and J. M. Wessels, *Adv. Mater.*, 2001, **13**, 1793–1797.
- 10 M. Mertig, L. C. Ciacchi, R. Seidel and W. Pompe, *Nano Lett.*, 2002, **2**, 841–844.
- 11 O. Harnack, W. E. Ford, A. Yasuda and J. M. Wessels, *Nano Lett.*, 2002, **2**, 919–923.
- 12 H. A. Becerril, R. M. Stoltenberg, C. F. Monson and A. T. Woolley, *J. Mater. Chem.*, 2004, **14**, 611–616.
- 13 C. F. Monson and A. T. Woolley, *Nano Lett.*, 2003, **3**, 359–363.
- 14 H. A. Becerril, R. M. Stoltenberg, D. R. Wheeler, R. C. Davis, J. N. Harb and A. T. Woolley, *J. Am. Chem. Soc.*, 2005, **127**, 2828–2829.
- 15 S. M. D. Watson, N. G. Wright, B. R. Horrocks and A. Houlton, *Langmuir*, 2010, **26**, 2068–2075.

- 16 L. Dong, T. Hollis, B. A. Connolly, N. G. Wright, B. R. Horrocks and A. Houlton, *Adv. Mater.*, 2007, **19**, 1748–1751.
- 17 A. Houlton, A. R. Pike, M. A. Galindo and B. R. Horrocks, *Chem. Commun.*, 2009, 1797–1806.
- 18 L. Dong, T. Hollis, S. Fishwick, B. A. Connolly, N. G. Wright, B. R. Horrocks and A. Houlton, *Chem.–Eur. J.*, 2007, **13**, 822–828.
- 19 M. Hocek and M. Fojta, *Org. Biomol. Chem.*, 2008, **6**, 2233–2241.
- 20 C. E. Arris, F. T. Boyle, A. H. Calvert, N. J. Curtin, J. A. Endicott, E. F. Garman, A. E. Gibson, B. T. Golding, S. Grant, R. J. Griffin, P. Jewsbury, L. N. Johnson, A. M. Lawrie, D. R. Newell, M. E. M. Noble, E. A. Sausville, R. Schultz and W. Yu, *J. Med. Chem.*, 2000, **43**, 2797–2804.
- 21 L. Jordheim, C. M. Galmarini and C. Dumontet, *Anticancer Drug Disc.*, 2006, **1**, 163–170.
- 22 A. M. Helguera, J. E. Rodriguez-Borges, X. Garcia-Mera, F. Fernandez, M. Natalia and D. S. Cordeiro, *J. Med. Chem.*, 2007, **50**, 1537–1545.
- 23 D. M. Huryn and M. Okabe, *Chem. Rev.*, 1992, **92**, 1745–1768.
- 24 E. De Clercq, *Antiviral Res.*, 2005, **67**, 56–75.
- 25 L. T. C. Franca, E. Carrilho and T. B. L. Kist, *Q. Rev. Biophys.*, 2002, **35**, 169–200.
- 26 H.-A. Wagenknecht, *Angew. Chem., Int. Ed.*, 2009, **48**, 2838–2841.
- 27 C. J. Yu, Y. Wan, H. Yowanta, J. Li, C. Tao, M. D. James, C. L. Tan, G. F. Blackburn and T. J. Meade, *J. Am. Chem. Soc.*, 2001, **123**, 11155–11161.
- 28 A. R. Pike, L. H. Lie, L. C. Ryder, B. R. Horrocks, W. Clegg, B. A. Connolly and A. Houlton, *Chem.–Eur. J.*, 2005, **11**, 344–353.
- 29 A. R. Pike, L. C. Ryder, B. R. Horrocks, W. Clegg, M. R. J. Elsegood, B. A. Connolly and A. Houlton, *Chem.–Eur. J.*, 2002, **8**, 2891–2899.
- 30 S. I. Khan, A. E. Beilstein and M. W. Grinstaff, *Inorg. Chem.*, 1999, **38**, 418–419.
- 31 H. Weizman and Y. Tor, *J. Am. Chem. Soc.*, 2001, **123**, 3375–3376.
- 32 M. Vrabel, R. Pohl, I. Votruba, M. Sajadi, S. A. Kovalenko, N. P. Ernsting and M. Hocek, *Org. Biomol. Chem.*, 2008, **6**, 2852–2860.
- 33 E. Meggers, P. L. Holland, W. B. Tolman, F. E. Romesberg and P. G. Schultz, *J. Am. Chem. Soc.*, 2000, **122**, 10714–10715.
- 34 G. H. Clever, K. Kaul and T. Carell, *Angew. Chem., Int. Ed.*, 2007, **46**, 6226–6236.
- 35 K. Tanaka, G. H. Clever, Y. Takezawa, Y. Yamada, C. Kaul, M. Shionoya and T. Carell, *Nat. Nanotechnol.*, 2006, **1**, 190–194.
- 36 C. T. Wirges, J. Timper, M. Fischler, A. S. Sologubenko, J. Mayer, U. Simon and T. Carell, *Angew. Chem., Int. Ed.*, 2009, **48**, 219–223.
- 37 K. Tanaka, A. Tengeji, T. Kato, N. Toyama and M. Shionoya, *Science*, 2003, **299**, 1212–1213.
- 38 I. Bouamaied, T. Nguyen, T. Ruhl and E. Stulz, *Org. Biomol. Chem.*, 2008, **6**, 3888–3891.
- 39 T. Nguyen, A. Brewer and E. Stulz, *Angew. Chem., Int. Ed.*, 2009, **48**, 1974–1977.
- 40 B. Datta, G. B. Schuster, A. McCook, S. C. Harvey and K. Zakrzewska, *J. Am. Chem. Soc.*, 2006, **128**, 14428–14429.
- 41 B. Datta and G. B. Schuster, *J. Am. Chem. Soc.*, 2008, **130**, 2965–2973.
- 42 W. Chen, M. Josowicz, B. Datta, G. B. Schuster and J. Janata, *Electrochem. Solid-State Lett.*, 2008, **11**, E11–E14.
- 43 W. Chen, G. Guler, E. Kuruvilla, G. B. Schuster, H. C. Chiu and E. Riedo, *Macromolecules*, 2010, **43**, 4032–4040.
- 44 H. He, J. Zhu, N. J. Tao, L. A. Nagahara, I. Amlani and R. Tsui, *J. Am. Chem. Soc.*, 2001, **123**, 7730–7731.
- 45 P. Nickels, W. U. Dittmer, S. Beyer, J. P. Kotthaus and F. C. Simmel, *Nanotechnology*, 2004, **15**, 1524–1529.
- 46 S. Pruneanu, S. A. F. Al-Said, L. Dong, T. A. Hollis, M. A. Galindo, N. G. Wright, A. Houlton and B. R. Horrocks, *Adv. Funct. Mater.*, 2008, **18**, 1–12.
- 47 R. Hassanien, M. Al-Hinai, S. A. F. Al-Said, R. Little, L. Siller, N. G. Wright, A. Houlton and B. R. Horrocks, *ACS Nano*, 2010, **4**, 2149–2159.
- 48 S. A. F. Al-Said, R. Hassanien, J. Hannant, M. A. Galindo, S. Pruneanu, A. R. Pike, A. Houlton and B. R. Horrocks, *Electrochem. Commun.*, 2009, **11**, 550–553.
- 49 A. R. Pike, L. H. Lie, R. A. Eagling, L. C. Ryder, S. N. Patole, B. A. Connolly, B. R. Horrocks and A. Houlton, *Angew. Chem., Int. Ed.*, 2002, **41**, 615–617.
- 50 A. R. Pike, S. N. Patole, N. C. Murray, T. Ilyas, B. A. Connolly, B. R. Horrocks and A. Houlton, *Adv. Mater.*, 2003, **15**, 254–258.
- 51 S. N. Patole, A. R. Pike, B. A. Connolly, B. R. Horrocks and A. Houlton, *Langmuir*, 2003, **19**, 5457–5463.

- 52 M. Vautrin, P. Leriche, A. Gorgues and M. P. Cava, *Electrochem. Commun.*, 1999, **1**, 233–237.
- 53 H. S. Nalwa, *Handbook of Advanced Electronic and Photonic Materials and Devices*, Academic Press, 2001.
- 54 S. Kotha and K. Singh, *Tetrahedron Lett.*, 2004, **45**, 9607–9610.
- 55 D. L. Meeker, D. S. K. Mudigonda, J. M. Osborn, D. C. Loveday and J. P. Ferraris, *Macromolecules*, 1998, **31**, 2943–2946.
- 56 F. von Kieseritzky, J. Hellberg, X. J. Wang and O. Inganas, *Synthesis*, 2002, 1195–1200.
- 57 J. P. Ferraris, R. G. Andrus and D. C. Hrcir, *J. Chem. Soc., Chem. Commun.*, 1989, 1318–1320.
- 58 F. H. Allen, *Acta Crystallogr., Sect. B: Struct. Sci.*, 2002, **58**, 380–388.
- 59 J. P. Conde, M. R. J. Elsegood and K. S. Ryder, *Acta Crystallogr., Sect. C: Cryst. Struct. Commun.*, 2004, **60**, 166–168.
- 60 K. Ogura, H. Yanai, M. Miokawa and M. Akazome, *Tetrahedron Lett.*, 1999, **40**, 8887–8891.
- 61 G. Cooke, J. F. Garety, B. Jordan, N. Kryvokhyzha, A. Parkin, G. Rabani and V. M. Rotello, *Org. Lett.*, 2006, **8**, 2297–2300.
- 62 S. Ghilgaber, W. N. Hunter and R. Marquez, *Tetrahedron Lett.*, 2007, **48**, 483–486.
- 63 M. J. Robins and P. J. Barr, *J. Org. Chem.*, 1983, **48**, 1854–1862.
- 64 C. McGuigan, C. J. Yarnold, G. Jones, S. Velazquez, H. Barucki, A. Brancale, G. Andrei, R. Snoeck, E. De Clercq and J. Balzarini, *J. Med. Chem.*, 1999, **42**, 4479–4484.
- 65 C. McGuigan, H. Barucki, S. Blewett, A. Carangio, J. T. Erichsen, G. Andrei, R. Snoeck, E. De Clercq and J. Balzarini, *J. Med. Chem.*, 2000, **43**, 4993–4997.
- 66 M. C. Etter, *Acc. Chem. Res.*, 1990, **23**, 120–126.
- 67 Z. A. Tehrani, A. Fattahi and A. Pourjavadi, *Carbohydr. Res.*, 2009, **344**, 771–778.
- 68 These findings do not appear to be an artifact/consequence of the particular equilibrium geometries. This was confirmed by running a series of single point calculations for the derivatives with different interplanar angles between the nucleobase and the pyrrolyl unit (0 – 180°). While some fluctuation in the spin density is observed the basic trend remains, *i.e.* the percentage of spin density on the pyrrolyl- decreases with increasing alkyl- chain length (see ESI† for details).
- 69 J. L. Bredas, G. B. Street, B. Themans and J. M. Andre, *J. Chem. Phys.*, 1985, **83**, 1323–1329.
- 70 A. Merz and F. Ellinger, *Synthesis*, 1991, 462–464.
- 71 N. Engel and W. Steglich, *Angew. Chem., Int. Ed. Engl.*, 1978, **17**, 676–676.
- 72 E. C. Taylor, J. E. Macor and J. L. Pont, *Tetrahedron*, 1987, **43**, 5145–5158.
- 73 Y. Saito, K. Matsumoto, S. S. Bag, S. Ogasawara, K. Fujimoto, K. Hanawa and I. Saito, *Tetrahedron*, 2008, **64**, 3578–3588.
- 74 L. Brandsma, O. A. Tarasova, N. A. Kalinina, A. I. Albanov, L. V. Klyba and B. A. Trofimov, *Russ. J. Org. Chem.*, 2002, **38**, 1073–1075.